HOSTED BY

ELSEVIER

CrossMark

Available online at www.sciencedirect.com

ScienceDirect

Progress in Natural Science: Materials International 25 (2015) 263–266

Progress in Natural Science Materials International

www.elsevier.com/locate/pnsmi
www.sciencedirect.com

Letter

New $(Fe_{0.76}Si_{0.09}B_{0.1}P_{0.05})_{98.25}Nb_1Cu_{0.75}$ bulk nanocrystalline alloys with good soft magnetic properties

Zongzhen Li[a], Shaoxiong Zhou[a,*], Chengliang Zhao[b], Lin Xue[b], Guangqiang Zhang[a], Rui Xiang[a]

[a]China Iron & Steel Research Institute Group, Advanced Technology & Materials Co., Ltd., Beijing 100081, China
[b]Key Laboratory of Magnetic Materials and Devices, Ningbo Institute of Materials Technology & Engineering, Chinese Academy of Sciences, 519 Zhuangshi Road, Zhenhai District, Ningbo, Zhejiang 315201, China

Received 27 March 2014; accepted 16 October 2014
Available online 2 July 2015

Abstract

A new $(Fe_{0.76}Si_{0.09}B_{0.1}P_{0.05})_{98.25}Nb_1Cu_{0.75}$ bulk nanocrystalline alloy in a rod shape with a diameter of 2.5 mm was successfully developed by copper mold casting and isothermal annealing. It was found that the introduction of Cu can result in the formation of a large number of α-Fe(Si) clusters (less than 3 nm) embedded in the glassy matrix, which greatly improved the primary crystallization of α-Fe(Si) nanocrystals during subsequent annealing. The obtained superior soft magnetic properties can be ascribed to the formation of optimal nanocomposite structures with a large number of α-Fe(Si) nanocrystals (~17 nm) uniformly distributed in the glassy matrix.

Keywords: Metallic glasses; Nanostructured materials; Rapid-solidification; Microstructure; TEM

1. Introduction

Nanocrystalline soft magnetic alloys have been widely used in common-mode power converters and power electronics [1–4]. Since these nanocrystalline alloys are usually made by crystallization of the corresponding amorphous alloys, the poor glass-forming ability (GFA) has limited the shape and dimension of these alloys to thin ribbons with a thickness less than 30 μm. In addition, the most commonly used commercial nanocrystalline alloy with the trade name Finemet has a rather low B_s value of 1.24 T [5]. It is therefore expected that the simultaneous improvement in their B_s and GFA to achieve high efficiency and miniaturization for electrical power and electronic devices and expand the field of their applications as bulk magnetic materials [1,2,6]. However, it is really difficult to achieve the combination of desired GFA and high B_s in one glassy alloy due to the following reasons: firstly, in order to obtain high GFA, a large number of glass-forming elements must be added, which reduces the Fe content accordingly and thus decreases B_s [7]; secondly, although Cu is good for the formation of high-density nucleation sites during annealing and is essential for the achievement of optimal microstructure of nanocomposite, the addition of Cu may also deteriorate GFA to some extent [8]; thirdly, the huge exothermic heat of crystallization of the bulk alloys during annealing may overheats the system to a high temperature, even much higher than their optimum temperature, leading to the rapid grain coarsening and overall deterioration of properties [9]. At present, there are a few reports about bulk nanocrystalline alloy, it is still necessary to develop new nanocrystalline alloys combined with high GFA and B_s for more extensive applications [10,11].

Recently, new FeSiBP bulk metallic glasses combined with high GFA and good soft magnetic properties were successfully developed [12]. High GFA allows for a decrease in the critical cooling rate of glass formation, which in turn enables the formation of the amorphous precursor phase. It is well known that the minor addition of Cu into glassy precursor alloys can greatly accelerate the formation of α-Fe(Si) nanocystals, and thus improve the soft magnetic properties [1,5,13]. In this investigation, by minor addition of Cu, newly modified

*Corresponding author. Tel.: +86 1062187216; fax: +86 1062182695.
E-mail address: sxzhou@atmcn.com (S. Zhou).
Peer review under responsibility of Chinese Materials Research Society.

http://dx.doi.org/10.1016/j.pnsc.2015.06.004

Finemet-type $(Fe_{0.76}Si_{0.09}B_{0.1}P_{0.05})_{98.25}Nb_1Cu_{0.75}$ bulk nanocrystalline alloy with an unusual combination of good magnetic properties and large GFA was synthesized to meet requirements for the real applications.

2. Experimental procedure

Alloy ingots with nominal compositions of $(Fe_{0.76}Si_{0.09}B_{0.1}P_{0.05})_{99-x}Nb_1Cu_x$ (x=0, and 0.75) were prepared by induction melting mixtures of Fe (99.99 mass%), Nb (99.9 mass %), Cu (99.99 mass%), crystalline B (99.5 mass%) and Si (99.99 mass%) metalloids and pre-alloyed Fe_3P (99.9 mass%) in a high-purity argon atmosphere. Cylindrical alloy rods with diameters up to 3.5 mm were fabricated by copper mold casting in air. The thermal properties were evaluated using the high sensitivity differential scanning calorimeter (DSC, NETZSCH 404C) in a high-purity argon flow. The samples were subjected to annealing at various temperatures for series time in an vacuum furnace and subsequently water quenching. The microstructures were characterized using X-ray Diffractometry (XRD, Bruker D8 Advance) with Cu-Kα radiation and a high-resolution transition electron microscopy (HRTEM, TECNAI F20). The average grain size of the nanocrystalline grains was estimated by using Scherrer equation from the full width at half maximum of the (110) reflection peak of body-centered cubic structure of α-Fe(Si). The saturation magnetic induction (B_s) was measured using a vibrating sample magnetometer (VSM, Lake Shore 7410) in a maximum applied field of 800 kA/m. All measurements were performed at room temperature.

3. Results and discussion

The XRD patterns of the as cast $(Fe_{0.76}Si_{0.09}B_{0.1}P_{0.05})_{99-x}Nb_1Cu_x$ (x=0, and 0.75) rods are shown in Fig. 1(a). The presence of only a broad diffuse peak at 2θ angle of $\sim 45^\circ$ confirms the amorphous nature of the alloys (x=0, and 0.75) with the critical diameters ranging from 2.5–3.5 mm. While the intensive crystalline diffraction peaks corresponding to α-Fe(Si) and Fe_3(B, and P) phases indicates the crystallization happened for the rod with diameter of 3 mm and Cu content of 0.75. Based on the XRD results, it is known that Cu addition reduces the GFA of $(Fe_{0.76}Si_{0.09}B_{0.1}P_{0.05})_{99-x}Nb_1Cu_x$ alloys, but the GFA for this alloy system with Cu content up to 0.75 is still large enough to fabricate an amorphous rod with a diameter of 2.5 mm. Fig. 1(b) shows the DSC curves of the as-cast $(Fe_{0.76}Si_{0.09}B_{0.1}P_{0.05})_{99-x}Nb_1Cu_x$ (x=0, and 0.75) ribbons with a diameter of 1 mm. With the introduction of Cu, the original single crystallization exothermic peak separates into three crystallization exothermic peaks, and the primary crystallization temperature T_{x1} shifts to a low temperature side. It is well known that the decrease of the primary crystallization temperature and the enlargement of ΔT ($\Delta T = T_{x_2} - T_{x_1}$) are obviously favorable for controlling the precipitation of α-Fe(Si) in the amorphous matrix [14]. Based on the XRD and DSC measurements shown in Fig. 1(a) and (b), it can be predicted that $(Fe_{0.76}Si_{0.09}B_{0.1}P_{0.05})_{98.25}Nb_1Cu_{0.75}$ alloy is suitable for fabricating bulk nanocrystalline alloy with high-density α-Fe(Si) nanoparticles.

The XRD patterns of the $(Fe_{0.76}Si_{0.09}B_{0.1}P_{0.05})_{98.25}Nb_1Cu_{0.75}$ rods with different diameters annealed at 550 °C for 10 min are shown in Fig. 2. The primary crystallization phase is identified to be α-Fe(Si) and the intensity of the diffraction peaks was enhanced with the increase of the average diameter of α-Fe(Si) nanoparticles. With the rod's diameter increased from 1 mm to 2.5 mm, the grain size of α-Fe (Si) has also enlarged from 17 nm to 21 nm. The increase of grain size may result from the higher temperature in the rods with the larger diameters caused by the exothermic heat of crystallization of the bulk alloys during annealing. The small change in the grain size implies the excellent thermal stability of this alloy.

The magnetic hysteresis loops and corresponding saturation magnetization M_s of $(Fe_{0.76}Si_{0.09}B_{0.1}P_{0.05})_{99-x}Nb_1Cu_x$ (x=0, and 0.75) rods annealed at 550 °C for 10 min are shown in Fig. 3. It can be seen that the annealed sample with Cu addition exhibits higher M_s of 1.54 T and slightly higher H_c of 1.9 A/m, compared with 1.43 T and 1.5 A/m for the Cu free glassy sample. The enhancement of M_s can be explained by the precipitation of α-Fe(Si) nanocrystals from the amorphous matrix [15–17]. It is well known that Cu element performs the role of nucleation agents during annealing. Introduction of Cu results in the precipitation of nano-sized α-Fe(Si) distributed widely in the amorphous matrix, giving rise to the volume of

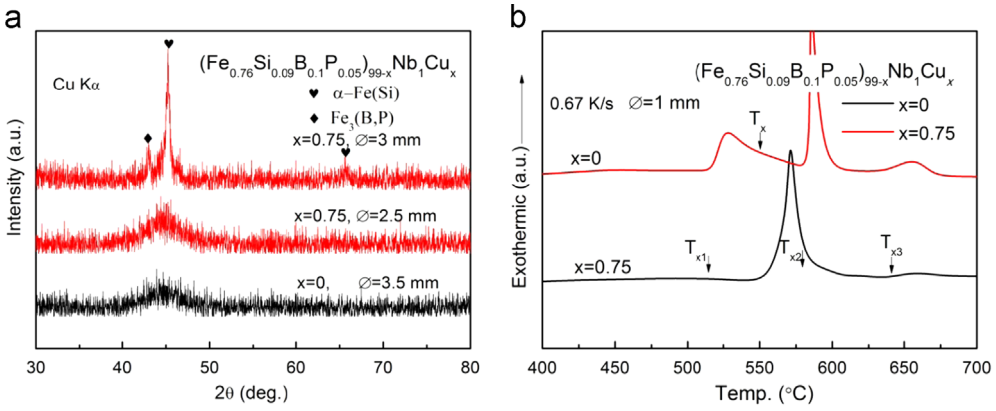

Fig. 1. (a) XRD patterns and (b) DSC curves of the as-cast $(Fe_{0.76}Si_{0.09}B_{0.1}P_{0.05})_{99-x}Nb_1Cu_x$ (x=0, and 0.75) rods.

fraction of the nano-sized α-Fe(Si) in the amorphous rods and leading to an obvious increase of B_s.

The TEM images taken from the $(Fe_{0.76}Si_{0.09}B_{0.1}P_{0.05})_{98.25}Nb_1Cu_{0.75}$ rods are shown in Fig. 4. The dispersion of a large number of clusters with grain size less than 3 nm in the glassy matrix was observed in the high resolution TEM image of the as-cast rod, and a diffused halo ring of (110) peaks of α-Fe(Si) was found in the corresponding SAED pattern inserted at right top corner of Fig. 4(a). Fig. 4(b) is the TEM image of the rod annealed at 550 °C for 10 min, showing random and condensed dispersion of the nanocrystals with average size of approximately 17 nm in the residual amorphous matrix. The SAED pattern inserted at the right top corner of Fig. 4(b) shows clearly the deflection rings of (110), (200) and (211) lattice planes of α-Fe (Si). In this case, the diffused halo ring pattern produced by the residual amorphous material is very weak.

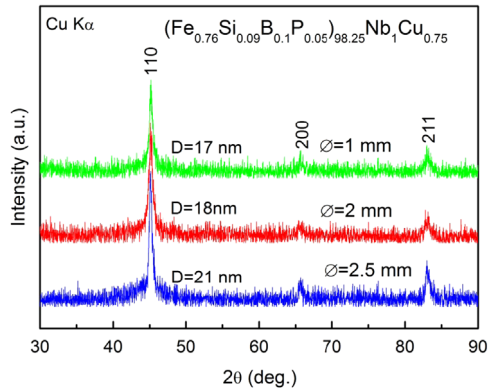

Fig. 2. XRD patterns of the as-cast $(Fe_{0.76}Si_{0.09}B_{0.1}P_{0.05})_{98.25}Nb_1Cu_{0.75}$ rods with diameter of 1 mm, 2 mm, and 2.5 mm annealed at 550 °C for 10 min, respectively.

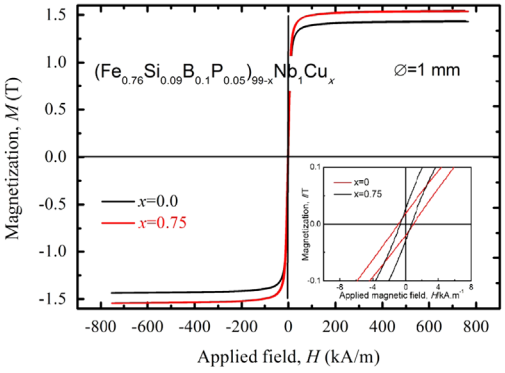

Fig. 3. DC hysteresis loops for $(Fe_{0.76}Si_{0.09}B_{0.1}P_{0.05})_{99-x}Nb_1Cu_x$ alloys. (x=0, and 0.75).

Based on the DSC, XRD and TEM results, the mechanism of the formation of $(Fe_{0.76}Si_{0.09}B_{0.1}P_{0.05})_{98.25}Nb_1Cu_{0.75}$ bulk nanocrystalline combined with excellent soft-magnetic properties and good thermal stability could be explained by the decrease of energy barrier for nucleation of α-Fe(Si) nanoparticles due to the addition of Cu. In the alloy without Cu addition, the energy barrier of α-Fe(Si) nucleation is so high that only a small amount of α-Fe(Si) grains could precipitate at the initial stage of crystallization. Fast coarsening of the α-Fe (Si) nanocrystals formed at the initial stage happened in the subsequent crystallization process and was responsible for the inferior soft magnetic properties of the $(Fe_{0.76}Si_{0.09}B_{0.1}P_{0.05})_{99}Nb_1$ nanocrystalline alloy. For the alloy with Cu addition, a large number of α-Fe(Si) clusters formed in the as cast state. The primary crystals may heterogeneously nucleate at the site of pre-existing α-Fe(Si) clusters during the primary crystallization. Nb atoms are rejected from the α-Fe(Si) phase and enriched in the amorphous matrix, which effectively depress the fast growth of the nanocrystals [18]. The steadily increasing nucleation rate creates more nucleis during the whole crystallization process. The competition during the growth of nuclei leads to the formation of fine and uniform grains of nano-size. As a consequence, the ferromagnetic exchange correlation between these grains significantly reduces the intrinsic magnetocrystalline anisotropy and contributes to superior soft magnetic properties.

4. Summary

In this letter, a new $(Fe_{0.76}Si_{0.09}B_{0.1}P_{0.05})_{98.25}Nb_1Cu_{0.75}$ bulk nanocrystalline rod with a large diameter of 2.5 mm

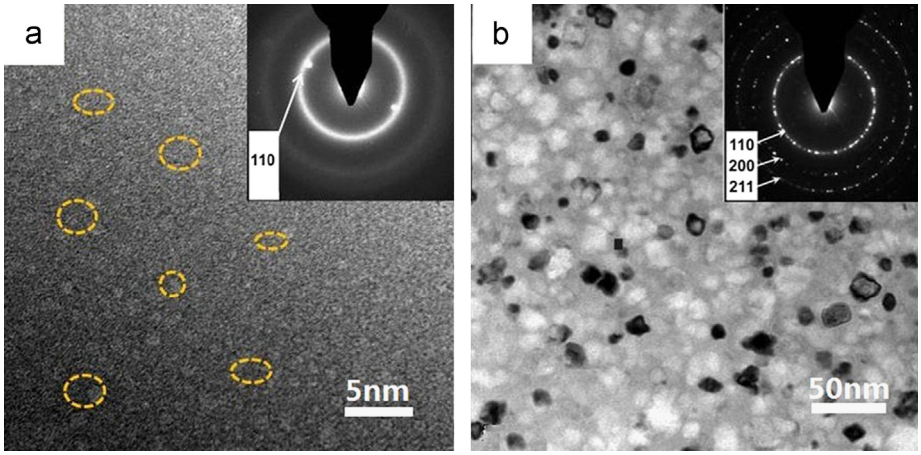

Fig. 4. The high-resolution TEM images and SAED patterns for $(Fe_{0.76}Si_{0.09}B_{0.1}P_{0.05})_{98.25}Nb_1Cu_{0.75}$ rods: (a) as cast, and (b) annealed at 550 °C for 10 min.

and good soft magnetic properties has been developed by properly adding Cu to $(Fe_{76}Si_9B_{10}P_5)_{99}Nb_1$ alloy. Introduction of Cu changes the crystallization process and stimulates the precipitation of α-Fe(Si) at lower temperature. The pre-existing clusters lead to uniform distribution of α-Fe(Si) in amorphous matrix. The $(Fe_{0.76}Si_{0.09}B_{0.1}P_{0.05})_{98.25}Nb_1Cu_{0.75}$ bulk nanocrystalline alloy with the modified microstructure exhibits high B_s of 1.54 T. The high B_s makes this bulk nanocrystalline alloy to be a potential magnetic material in industry applications.

Acknowledgments

This work was supported by the National Natural Science Foundation of China (Grant no. 51341002), the Beijing Municipal Science and Technology Project (Grant no. Z141100003814007), and the National Key Technology R&D Program (Grant no. 2013BAE08B01).

References

[1] G. Herzer, Acta Mater. 61 (2013) 718–734.
[2] R. Hasegawa, J. Magn. Magn. Mater. 324 (2012) 3555–3557.
[3] M. Ohta, Y. Yoshizawa, J. Phys. D: Appl. Phys. 44 (2011) 064004.
[4] M. Ohta, Y. Yoshizawa, Jpn. J. Appl. Phys. 46 (2007) L477–L479.
[5] Y. Yoshizawa, S. Oguma, K. Yamauchi, J. Appl. Phys. 64 (1988) 6044–6046.
[6] A. Urata, H. Matsumoto, S. Sato, A. Makino, J. Appl. Phys. 105 (2009) 07A323–07A324.
[7] J. Schroers, Phys. Today 66 (2013) 32.
[8] X. Li, H. Kato, K. Yubuta, A. Makino, A. Inoue, Mater. Sci. Eng.: A 527 (2010) 2598–2602.
[9] T.-S. Chin, C. Lin, M. Lee, R. Huang, S. Huang, Intermetallics 16 (2008) 52–57.
[10] A. Inoue, B. Shen, J. Mater. Res. 18 (2003) 2799–2806.
[11] Z. Li, A. Wang, C. Chang, Y. Wang, B. Dong, S. Zhou, Intermetallics 54 (2014) 225–231.
[12] C. Chang, C. Qin, A. Makino, A. Inoue, J. Alloy. Compd. 533 (2012) 67–70.
[13] Z. Li, S. Zhou, Y. Wang, R. Xiang, G. Zhang, Mater. Lett. 148 (2015) 99–102.
[14] T. Kubota, A. Makino, A. Inoue, J. Alloy. Compd. 509 (Supplement 1) (2011) S416–S419.
[15] Z. Li, A. Wang, C. Chang, Y. Wang, B. Dong, S. Zhou, J. Alloy. Compd. 611 (2014) 197–201.
[16] L. Xue, H. Liu, L. Dou, W. Yang, C. Chang, A. Inoue, X. Wang, R.-W. Li, B. Shen, Mater. Des. 56 (2014) 227–231.
[17] A. Wang, H. Men, B. Shen, G. Xie, A. Makino, A. Inoue, Thin Solid Films 519 (2011) 8283–8286.
[18] C. Smith, S. Katakam, S. Nag, Y. Zhang, J. Law, R.V. Ramanujan, N. B. Dahotre, R. Banerjee, Metall. Mater. Trans. A 45 (2014) 2998–3009.